HHS Public Access

Author manuscript

Nat Microbiol. Author manuscript; available in PMC 2019 April 16.

Published in final edited form as:

Nat Microbiol. 2018 September ; 3(9): 996–1009. doi:10.1038/s41564-018-0215-6.

N^{e}-fatty acylation of multiple membrane-associated proteins by *Shigella* IcsB effector to modulate host function

Wang Liu[1,2,3,9], **Yan Zhou**[3,4,8,9], **Tao Peng**[5,6,9], **Ping Zhou**[3], **Xiaojun Ding**[3], **Zilin Li**[3], **Haoyu Zhong**[3], **Yue Xu**[3], **She Chen**[3], **Howard C. Hang**[6,*], and **Feng Shao**[3,7,*]

[1]College of Life Science, Peking University, Beijing, China.

[2]Peking University–Tsinghua University–National Institute of Biological Sciences Joint Graduate Program, National Institute of Biological Sciences, Beijing, China.

[3]National Institute of Biological Sciences, Beijing, China.

[4]College of Life Sciences, Beijing Normal University, Beijing, China.

[5]School of Chemical Biology and Biotechnology, Peking University Shenzhen Graduate School, Shenzhen, China.

[6]Laboratory of Chemical Biology and Microbial Pathogenesis, The Rockefeller University, New York, NY, USA.

[7]Tsinghua Institute of Multidisciplinary Biomedical Research, Tsinghua University, Beijing, China.

[8]Present address: Life Sciences Institute and Innovation Center for Cell Signaling Network, Zhejiang University, Hangzhou, Zhejiang, China.

[9]These authors contributed equally: Wang Liu, Yan Zhou, Tao Peng.

Abstract

Shigella flexneri, an intracellular Gram-negative bacterium causative for shigellosis, employs a type III secretion system to deliver virulence effectors into host cells. One such effector, IcsB, is

[*]**Correspondence and requests for materials** should be addressed to H.C.H. or F.S. hhang@mail.rockefeller.edu; shaofeng@nibs.ac.cn.

Author contributions

F.S. conceived the study. Y.Z. performed initial studies on the identification of RhoGTPases as the substrate of IcsB and its fatty acyltransferase activity. W.L. established the SunTag labelling of T3SS effectors, analysed the proteomic hits of IcsB, and performed the localization and autophagy studies. P.Z. and Z.L. provided technical assistance to Y.Z. and W.L. H.Z. and Y.X. performed the plaque assay. T.P. and H.C.H. were responsible for the chemical proteomic analyses. X.D. and S.C. carried out the mass spectrometry experiments. Y.Z., W.L., T.P., S.C., H.C.H. and F.S. analysed the data. W.L., Y.Z. and F.S. wrote the manuscript. All authors discussed the results and commented on the manuscript.

Competing interests

The authors declare no competing interests.

Reporting Summary. Further information on experimental design is available in the Nature Research Reporting Summary linked to this article.

Data availability. The data that support the findings of this study are included in this published article along with its Supplementary Information files, and are also available from the corresponding author upon request.

Additional information

Supplementary information is available for this paper at https://doi.org/10.1038/s41564-018-0215-6.

Publisher's note: Springer Nature remains neutral with regard to jurisdictional claims in published maps and institutional affiliations.

critical for *S. flexneri* intracellular survival and pathogenesis, but its mechanism of action is unknown. Here, we discover that IcsB is an 18-carbon fatty acyltransferase catalysing lysine N^{ε}-fatty acylation. IcsB disrupted the actin cytoskeleton in eukaryotes, resulting from N^{ε}-fatty acylation of RhoGTPases on lysine residues in their polybasic region. Chemical proteomic profiling identified about 60 additional targets modified by IcsB during infection, which were validated by biochemical assays. Most IcsB targets are membrane-associated proteins bearing a lysine-rich polybasic region, including members of the Ras, Rho and Rab families of small GTPases. IcsB also modifies SNARE proteins and other non-GTPase substrates, suggesting an extensive interplay between *S. flexneri* and host membrane trafficking. IcsB is localized on the *Shigella*-containing vacuole to fatty-acylate its targets. Knockout of CHMP5—one of the IcsB targets and a component of the ESCRT-III complex—specifically affected *S. flexneri* escape from host autophagy. The unique N^{ε}-fatty acyltransferase activity of IcsB and its altering of the fatty acylation landscape of host membrane proteomes represent an unprecedented mechanism in bacterial pathogenesis.

Bacterial pathogens have sophisticated interplay with their host to promote infection and cause diseases. A critical virulence mechanism commonly used by different pathogens is to secrete effectors or toxins that manipulate various host processes. Many Gram-negative bacteria have evolved a type III secretion system (T3SS) to deliver multiple effectors into host cytosol. These effectors are often endowed with unique and potent biochemical activities to post-translationally modify host proteins[1]. *Shigella flexneri* is an enteropathogenic bacterium that causes bacillary dysentery by invasion and spread through the colonic epithelium[2]. *S. flexneri* deploys more than a dozen T3SS effectors to modulate host immune responses, cytoskeleton dynamics and vesicle trafficking[3,4]. Revealing the mechanism of these effectors not only advances the understanding of bacterial infection, but can also lead to the discovery of new enzymatic post-translational modifications. For example, OspF and its homologous effectors in other bacteria harbour an unprecendented phosphothreonine lyase activity that catalyses elimination of the phosphothreonine in MAPKs to block host immunity[5–8].

IcsB—one of the first identified *Shigella* T3SS effectors[9]—modulates several host cellular processes, including lysis of the protrusions during *S. flexneri* intercellular spread[9,10], evasion of host autophagy[11–13] and avoiding septin cage entrapment[14]. The Δ*icsB* mutant is deficient in provoking keratoconjunctivitis in infected guinea pigs, indicating its critical role in *S. flexneri* pathogenicity. Various models are proposed to account for the functional mechanism of IcsB[11,13–15], but the host target(s) that can explain its pleiotropic functions are not identified. While bioinformatic analyses have indicated a possible enzyamtic activity in IcsB[16], whether and how IcsB employs a catalytic mechanism to modulate its host target(s) remains unknown.

Here, we discover that IcsB is an 18-carbon fatty acyltransferase that can modify RhoGTPases and disrupt their membrane cycling. The modification occurs on the ε -NH_2 group of several lysines in the polybasic region (PBR) preceding the prenylated cysteine. Chemical proteomics identify about 60 IcsB substrates, including members of the Ras, Rho and Rab families of small GTPases and other membrane trafficking proteins. We further

observe that CHMP5—a substrate of IcsB and a component of the endosomal sorting complex required for transport III (ESCRT-III) complex—is essential for anti-*Shigella* autophagy. Our work demonstrates that long-chain N^{ε}-fatty acylation, which rarely occurs in eukaryotes, is exploited by the pathogen to alter the acylation landscape of host proteomes and manipulate host defences.

Results

The putative catalytic motif in IcsB is critical for its functioning.

Saccharomyces cerevisiae is a useful model for elucidating the molecular function of bacterial effectors. We found that inducible expression of IcsB could severely block *S. cerevisiae* growth (Fig. 1a). The cytotoxicity was also observed in IcsB-transfected 293T cells (Fig. 1b). IcsB is present in all four pathogenic *Shigella* species (*S. flexneri*, *S. sonnei*, *S. dysenteriae* and *S. boydii*), and shares about 24% sequence homology with the *Burkholderia pseudomallei* T3SS effector BopA as well as the RID (Rho-inactivation domain) domain of *Vibrio* species multifunctional autoprocessing repeats-in-toxin (MARTX) toxins (Fig. 1c). The three proteins adopt a similar secondary structure arrangement[16] (Fig. 1c). Previous bioinformatics analysis identifies His-145, Asp-195 and Cys-306 in IcsB that are conserved in BopA and RID (Fig. 1c), which may form a catalytic triad resembling that in the circularly permuted papain-like hydrolytic enzymes[16,17]. Alanine substitution of His-145, Asp-195 or Cys-306 in IcsB diminished its cytotoxicity in yeast, while mutation of two other residues (K183A and Y297A) had no effect (Fig. 1a). Similar findings were obtained in IcsB-transfected 293T cells (Fig. 1b). *icsB* is critical for *S. flexneri* intercellular spread, particularly in the absence of *virA*[9,10,15]. We confirmed this virulence defect caused by Δ*icsB* in *S. flexneri* 2457T (Supplementary Fig. 1a), as well as the requirement of the His–Asp–Cys triad of IcsB (Supplementary Fig. 1b,c). Thus, IcsB and its homologous effectors may function as a papain-like hydrolytic enzyme in modulating host function.

IcsB disrupts the actin cytoskeleton by inactivating RhoGTPases.

IcsB expression could disrupt the actin cytoskeleton in HeLa cells, as is evident from the loss of filamentous actin fibres and the development of cell-rounding responses (Fig. 1d). Such activity was also blocked by mutation of any residue in the His–Asp–Cys motif. The cytoskeleton phenotype caused by IcsB resembles that of the *Yersinia* T3SS effector YopT[18]. YopT is a papain-like cysteine protease that cleaves the carboxy (C)-terminal prenylated cysteine in Rho family small GTPases (RhoA, Rac1 and Cdc42). Notably, the RID of MARTX toxin can also disrupt the actin cytoskeleton by inactivating RhoGTPases[19], which requires the His–Asp–Cys motif[17] (rather than the His–Tyr–Cys motif proposed in the bioinformatics analysis[16]). Consistent with these observations, IcsB expression could diminish the interaction of RhoA Q63L (a mutant locked in the GTP-bound form) with its effector domain RBD (Rho-binding domain of Rhotekin), dependent on the Cys-306 (Supplementary Fig. 2a). IcsB also disrupted the interaction between RhoA and Rho GDP-dissociation inhibitor (RhoGDI), which was abolished by mutations of the His–Asp–Cys motif but not Tyr-297 (Supplementary Fig. 2b). Thus, IcsB uses its papain-like activity to inactivate RhoA in mammalian cells.

IcsB disrupts RhoGTPase membrane cycling by modifying its C-terminal tail.

The fact that IcsB could block the RhoA–GTP interaction with RhoGDI indicates that IcsB, like YopT, may modulate RhoGTPase cycling onto and off the membrane. Consistent with this idea, IcsB expression abolished the precipitation of Rac1/Cdc42 Q61L (equivalent to RhoA Q63L) by RhoGDI while it had no effect on their binding to the effector domain PBD (The Rac/Cdc42 (p21)-binding domain of PAK-1 protein) (Supplementary Fig. 2c,d). When the prenylated Cys-190 in RhoA was mutated into alanine, its precipitation by the RBD resisted disruption by IcsB (Supplementary Fig. 2e). These results indicate that IcsB inhibition of RhoA–RBD binding is an indirect result of the alteration of RhoA membrane association. The prenylated RhoGTPase is prone to be partitioned into the detergent phase in the Triton X-114 partitioning assay. Overexpressed RhoA was partitioned into both the aqueous and the detergent phase[18], but IcsB treatment of the cell lysates led to RhoA partitioning exclusively into the detergent phase (Fig. 2a). Thus, the action of IcsB increases the hydrophobicity and membrane association of RhoA. YopT treatment abolishes RhoA partitioning into the detergent phase[18]. Using this assay, we observed that RhoA from IcsB but not IcsB C306A mutant-transfected cells resisted YopT cleavage (Fig. 2b). Similar results were obtained with Rac1 and Cdc42 (Fig. 2b).

RhoGTPases are frequently targeted by bacterial pathogens[20], which is often mediated by bacterial toxins or effector-catalysed covalent modifications. In vitro pulldown of recombinant MBP (maltose-binding protein)-IcsB C306A from bovine brain extracts identified a specific binding partner of 25 kDa (Fig. 2c), and this band mainly contained Rho, Rac1 and Cdc42, according to mass spectrometry identification. Confirming this observation, RhoA was readily co-immunoprecipitated by IcsB from transfected 293T cells (Fig. 2d). Furthermore, endogenous RhoA in 293T cells often showed a slow migration on a high-concentration sodium dodecyl sulfate polyacrylamide gel electrophoresis (SDS-PAGE) gel upon expression of IcsB, but not IcsB C306A (Fig. 2e). Thus, IcsB probably directly modifies RhoGTPases, rendering them more hydrophobic.

The C-terminal tail of RhoA, bearing the prenylated cysteine, is sufficient for recognition and cleavage by YopT[18,21]. Expression of IcsB, but not IcsB C306A, rendered the enhanced green fluorescent protein (eGFP)-tagged RhoA C-terminal tail resistant to YopT cleavage (Fig. 2f). The tail, when co-expressed with IcsB in 293T cells, exhibited a more evident mobility shift (Fig. 2g). PDEδ, a non-selective prenyl-binding protein, could efficiently pull down RhoA from cell lysates, but this was not altered by IcsB expression (Fig. 2h). Taken together, these data suggest that IcsB probably modifies the C-terminal tail of RhoA without affecting its prenylation.

IcsB is an 18-carbon *N*-fatty acyltransferase that modifies lysine residues in the C-terminal PBR in RhoGTPases.

To reveal the modification on RhoA, we affinity-purified Flag-RhoA Q63L from control or IcsB-expressing cells and performed mass spectrometry analyses. Determination of the total molecular mass revealed that RhoA was modified with 1, 2 or 3 18-carbon fatty acyl groups (stearoyl or oleoyl) (Fig. 3a). Tandem mass spectrometry (MS/MS) analysis showed that the acyl groups were conjugated to Lys-185, Lys-186 and Lys-187 in the PBR of RhoA (Fig.

3b–d). The PBR, preceding the prenylated cysteine, has electrostatic interactions with phospholipid head groups in the membrane. Thus, fatty acylation of the PBR increased the hydrophobicity and membrane association of RhoA (Fig. 2a). The modification also explains the resistance of IcsB-modified RhoA to YopT cleavage, as an intact PBR is required for recognition by YopT[18,21]. According to the crystal structure of RhoGDI complexed with prenylated Cdc42 (ref. [22]), fatty acylation of the PBR should disrupt the binding of RhoGDI to RhoGTPases, also explaining our experimental observations (Supplementary Fig. 2b,d).

We attempted to reconstitute IcsB fatty acylation of RhoA in vitro. Purified farnesylated RhoA (the L193S mutant was used to switch the native geranylgeranylation to farnesylation), obtained from coexpression with the farnesyltransferase (FTase) in *Escherichia coli*, was incubated with recombinant MBP-IcsB in the presence of H^3-stearoyl-CoA and inositol hexaphosphate (IP_6). Autoradiography showed that the GTPase was readily modified by the stearoyl group, which did not occur with IcsB C306A (Fig. 3e). We also performed the same reaction using cold stearoyl-CoA. Mass spectrometry then revealed that the molecular mass of RhoA was increased by 535 and 801 Da (Supplementary Fig. 3a), corresponding to the addition of 2 and 3 stearoyl groups, respectively. MS/MS analyses confirmed the modification on Lys-185, Lys-186 and Lys-187 (Supplementary Fig. 3b,c). The *Yersinia* T3SS effector YopJ, which also bears a papainlike hydrolytic triad, acetylates serine and threonine residues in MAPK kinases[23]. Different from YopJ, IcsB is an 18-carbon fatty acyltransferase that modifies lysine residues. IcsB-catalysed modification also differs from the known long-chain fatty acylation that generally occurs on a cysteine or the amino (N) terminus of a glycine residue.

We found that the C-terminal tail of RhoA expressed in the absence of the FTase resisted modification by IcsB and was therefore only partitioned into the aqueous phase (Fig. 3f). Consistently, IcsB did not affect the activation state of non-prenylated RhoA C190A (Supplementary Fig. 2e). Thus, prenylation of RhoA is required for its recognition by IcsB. Moreover, IcsB-catalysed H^3-stearoyl labelling of RhoA was barely detectable in the absence of IP_6 (Fig. 3e). This property echoes several other bacterial toxins, including the autoprocessing cysteine protease domain of the large clostridial cytotoxins TcdA and TcdB[24] and the *Vibrio* MARTX toxin[25], and a cysteine protease domain-like T3SS effector from *V. parahaemolyticus*[26], as well as the YopJ family of acetyltransferase effectors[27]. A previous study reported a cholesterol-binding region in IcsB[12], but cholesterol was not required for IcsB stearoylation of RhoA in vitro.

Stearoylome profiling reveals that IcsB modifies multiple host proteins.

The fact that IcsB can target the prenylated C-terminal tail of RhoA without full-length RhoA indicates that IcsB may modify other host proteins. We therefore employed bioorthogonal chemical proteomics[28,29] to profile IcsB-fatty-acylated proteins in living cells. Specifically, HeLa cells were labelled with alk-16—an alkyne analogue of stearic acid that can be metabolized and covalently installed onto cellular proteins[30,31]. Alkyne-labelled proteins in cell lysates were then subjected to the click-chemistry reaction with azide-rhodamine for in-gel fluorescence, or azide-biotin for streptavidin enrichment and mass

spectrometry. In the pilot in-gel fluorescence assay, several abundant stearoylated proteins were detected specifically in the lysates of cells expressing wild-type (WT) IcsB (Fig. 4a). To quantify the differences in stearoylated proteins between WT IcsB and IcsB C306A-expressing cells, double SILAC (stable isotope labelling with amino acids in cell culture) proteomic analyses were also performed (Supplementary Fig. 4a). The quantification identified about 60 proteins that were stearoylated in an IcsB-dependent manner (Fig. 4b, Table 1 and Supplementary Table 1), most of which belong to the Ras superfamily of small GTPases, including the Ras family (R-Ras, K-Ras, H-Ras, Rap1B, RalA, RalB and RheB), Rho family (Rac1, Rac2, RhoA, RhoC and RhoG) and Rab family (Rab1A, Rab5B, Rab8A, Rab10, Rab11A, Rab11B, Rab13, Rab22A, Rab23, Rab34 and Rab35). The list also contains non-small GTPase proteins, including SNARE proteins (YKT6, VAMP3, VAMP8, SEC22B and BNIP1/SEC20), *N*-myristoylated proteins (MARCKS, MARCKSL1 and BASP1), septins (SEPT7 and SEPT11) and some other proteins. Gene Ontology-based clustering analysis suggested that these proteins regulate the actin cytoskeleton, membrane trafficking, cell–cell adherens junctions, and endocytosis and endosomal recycling (Supplementary Fig. 4b).

We also performed the proteomic profiling under *S. flexneri* infection conditions. For this, HeLa cells were infected with the *icsB*-sufficient or -deficient *S. flexneri* strains. An evident increase of total stearoylated proteins was observed with *icsB*-positive infections (Fig. 4a). SILAC quantitative proteomics identified more than 40 proteins that were stearoylated in an *icsB*-dependent manner (Fig. 4b). The presence or absence of VirA, which affects autophagy of intracellular *S. flexneri*[32], had little influence on the stearoylated proteins identified (Fig. 4b). The list of stearoylated proteins during infection largely overlapped with that of the transfection experiment (Table 1 and Supplementary Table 2). In-gel fluorescence assay of a dozen selected candidates, including small GTPases (Rho, Ras, Rap and Rab) and the non-small GTPase protein VAMP8 showed that they could all be labelled with azide-rhodamine upon *icsB*-positive infections (Fig. 4c), validating the proteomic data. Thus, IcsB alters the fatty acylation landscape of the host cell proteome to modulate multiple host cellular processes.

Using the alk-16 labelling assay, we found that only mutations of all three lysines (Lys-185, Lys-186 and Lys-187) in the PBR of RhoA could completely block its stearoylation by IcsB in 293T cells (Fig. 4d). Results of a similar nature were obtained with VAMP8 and Rab13—two other IcsB substrates that also have a PBR preceding their C-terminal membrane insertion or association sequences (Fig. 4d).

IcsB is localized on *Shigella*-containing vacuoles and modifies its substrates there.

The substrates of IcsB are all known to be membrane associated or within a membrane complex (Table 1 and Fig. 5a). Consistently, ectopically expressed IcsB in 293T cells was in the membrane fraction (Fig. 5b). To investigate the localization of IcsB during *S. flexneri* infection, we used the recently developed SunTag system, which is extremely sensitive in imaging a cellular protein tagged with a GCN4 protein-derived peptide (SunTag)[33,34]. Specifically, eGFP-fused single-chain anti-SunTag antibody was stably expressed in HeLa cells, and the cells were then infected with *S. flexneri* expressing IcsB harbouring 24 copies

of the SunTag. The 24× SunTag did not affect T3SS-dependent secretion of IcsB (Supplementary Fig. 5a). The data revealed that T3SS-delivered IcsB, before bacterial escape from the vacuole into the cytosol, was localized on *S. flexneri*-containing vacuole membranes (Fig. 5c,d).

Many of the IcsB substrates, including the Ras superfamily of small GTPases, rely on their C-terminal cysteine prenylation to be membrane associated. Serine substitution of the cysteine in representative members of the Rho, Ras, Rab and Rap families abolished their stearoylation by transfected IcsB in 293T cells (Fig. 5e). Similar results were obtained with a prenylated non-GTPase substrate CNP, a microtubule-associated 2′, 3′ -cyclic nucleotide-3′ -phosphodiesterase (Fig. 5e). Deletion of the C-terminal transmembrane domain in VAMP8 also diminished its stearoylation by IcsB (Fig. 5e). The membrane insertion motif in these IcsB substrates is often preceded by a PBR (Fig. 5f). We generated PBR-mutated RhoA, Rab13 and VAMP8 containing only one lysine, with all other lysines mutated into arginine (with PBR) or with all other lysines or arginines mutated into alanine (without PBR). Mutations to alanine abolish or reduce the membrane association. When subjected to IcsB-catalysed stearoylation in cells, the one-lysine-with-PBR mutants were still modified by IcsB, in contrast with their cognate-without-PBR mutants (Fig. 5f). Thus, membrane localization of IcsB targets is required for their encounter with and subsequent fatty acylation by IcsB from *S. flexneri*.

Fatty acylation of CHMP5 by IcsB is important for *Shigella* evasion of autophagy.

Loss of *icsB* in *S. flexneri* results in trapping of the bacterium into the autophagosome[11–13,15]. We confirmed that few WT *S. flexneri* were positive for the autophagosome marker eGFP-LC3 while nearly 80% of Δ*icsB* -infected cells contained eGFP-LC3-decorated bacteria (Supplementary Fig. 5b,c). The increased autophagy of *S. flexneri* Δ*icsB* was suppressed by expression of WT IcsB, but not its acyltransferase-inactive H145A, D195A and C306A mutants in the bacteria (Supplementary Fig. 5b,c). As expected, eGFP-LC3 decoration of *S. flexneri* Δ*icsB* was diminished in *ATG16*$^{-/-}$ or *ATG5*$^{-/-}$ HeLa cells (Supplementary Fig. 5d,e). It is necessary to note that the impact of IcsB deficiency on anti-*Shigella* autophagy was not that robust, particularly when the percentage of intracellular bacteria decorated with eGFP-LC3 was counted. Thus, the overall relevance of IcsB inhibition of autophagy to *Shigella* pathogenesis requires further investigation, which is consistent with our finding of IcsB targeting of multiple different host proteins.

To investigate whether any IcsB substrate is involved in *S. flexneri* autophagy, knockout or knockdown analyses in HeLa cells were performed with nearly all the substrates identified from the proteomic screen. These extensive analyses (Table 1) only identified one gene, *CHMP5* (charged MVB protein 5), whose deficiency could inhibit eGFP-LC3 decoration of *S. flexneri* Δ*icsB* (Fig. 6a,b and Supplementary Fig. 6a,b). The defective autophagy of *S. flexneri* Δ*icsB* was restored by re-expression of CHMP5 in the knockout cells. Consistent with the functional data, CHMP5 was found to be stearoylated by IcsB in *S. flexneri*-infected 293T cells (Fig. 6c). The N-terminal region in CHMP5 contains three lysines (Lys-7, 9 and 11) and one arginine (Arg-3), resembling the PBR in other IcsB substrates. Mutation of Lys-7 or the three lysines together severely inhibited or completely blocked

CHMP5 stearoylation by IcsB, respectively (Fig. 6d), whereas mutation of other lysine residues in CHMP5 showed no effects (Supplementary Fig. 7a). Thus, IcsB mainly targets Lys-7 in CHMP5 for stearoylation, resulting in suppression of antibacterial autophagy in host cells. CHMP5 is a component of the ESCRT-III complex[35,36]. *CHMP5*$^{-/-}$ did not affect *S. flexneri* invasion into HeLa cells (Supplementary Fig. 6c,d). Thus, CHMP5 is probably involved in regulating the trafficking and property of *S. flexneri*-containing vacuoles, which indirectly affects development of the autophagic response to *S. flexneri*. Supporting this notion, *CHMP5*$^{-/-}$ in HeLa cells disrupted autophagosome formation in response to both Δ*icsB* and WT *S. flexneri* infection (Fig. 6a,b). Endogenous CHMP5 could be identified on *Shigella*-containing vacuoles (Fig. 6e).

We also infected *CHMP5*$^{-/-}$ HeLa cells with other bacterial pathogens, including *Salmonella typhimurium*, *Yersinia pseudotuberculosis* (the effector-less Δ HEMOJ(T) IP2666 strain) or *Listeria monocytogenes*, which are known to be targeted by host autophagy. Interestingly, eGFP-LC3 decoration of these bacteria was not affected by the loss of *CHMP5* (Supplementary Fig. 7b,c). This agrees with the hypothesis that CHMP5 and the ESCRT-III complex may have a differential role in endocytosis-mediated entry for different bacteria. Thus, CHMP5 functions specifically in anti-*Shigella* autophagy, and its fatty acylation by IcsB contributes to *Shigella* escape from host autophagy.

Discussion

In summary, we show that the T3SS effector IcsB from *S. flexneri* targets a large set of host proteins for fatty acylation during infection. This property differs from other bacterial effectors that often act on one or a few host proteins. Most IcsB targets, such as the small GTPases, bear the CAAX-mediated prenylation. IcsB modifies RhoGTPases and disrupts their membrane cycling, which causes cell rounding in transfected cells, but not in *S. flexneri*-infected cells. This is different from the RID of MARTX toxin whose inactivation of Rho causes cell rounding during infection[19]. It is possible that IcsB modification of RhoGTPases is not extensive enough to generate a gross cytoskeleton phenotype. Thus, the functional consequence of IcsB modification of its other targets during infection is a subject of future studies. Despite this, IcsB appears to be a master effector that alters the fatty acylation landscape of host membrane proteomes during *S. flexneri* infection.

Autophagy is important for host defence against bacterial infections[37]. Different bacterial pathogens enter the host cell through different routes with distinct trafficking routes. Successful pathogens have evolved effectors to hijack different steps in bacterial autophagy. The *Legionella pneumophila* RavZ effector cleaves and deconjugates LC3-PE (LC3-phosphatidylethanolamine conjugate)[38]. *S. flexneri* VirA inactivates Rab1 at the endoplasmic reticulum–Golgi exit sites to block autophagosome membrane formation[32]. We show that IcsB modifies the endosomal ESCRT-III complex protein CHMP5, and *CHMP5* deficiency suppresses anti-*Shigella* autophagy. These results suggest that IcsB functions during the trafficking of endosome-derived *Shigella*-containing vacuoles, and its suppression of autophagy is an indirect result of CHMP5 inactivation. CHMP5 deficiency does not affect autophagy of other intracellular bacteria, consistent with the distinct endosomal machineries exploited by different bacteria.

Fatty acylation modification is present in all kingdoms of life, and long-chain fatty acylation is commonly manifested as *N*-myristoylation and *S*-palmitoylation of the N-terminal glycine and cysteine residues, respectively[39–41]. Lysine N^{ε}-fatty acylation has only been found on aquaporin-0 (ref. [42]) and some secreted cytokines[40,43,44], but their functional significance is unclear. IcsB catalyses N^{ε}-fatty acylation to modulate multiple host cellular processes. IcsB adopts a papain-like fold that is common in the protein structure space. It is not unexpected that N^{ε}-fatty acylation might be widely used in regulating eukaryotic biology. A recent study shows that SIRT6 can defatty-acylate PBR lysines in R-Ras2[45]. While our manuscript was under revision, a follow-up study reported that the RID of MARTX toxin also functions as a long-chain N^{ε}-fatty acyltransferase to modify PBR lysine residues of RhoGTPase[46], which explains the known functions of RID, such as inducing host cell rounding and inhibiting phagocytosis17,19,47.

Methods

Plasmids, antibodies and reagents.

DNA for the *icsB* gene was amplified from the genomic DNA of the *S. flexneri* 2a strain 2457T. For recombinant expression in *E. coli*, *icsB* DNA was constructed into the pSUMO vector with an N-terminal SUMO (small ubiquitin-like modifier) tag and the pMal vector with an N-terminal MBP tag. For expression in mammalian cells, *icsB* DNA was cloned into the pCS2 vector with an N-terminal 3× Flag tag or a modified peGFP-C1 or pLKO1 vector containing a Flag tag preceding eGFP. *ipgA* DNA was cloned into the pCS2 vector with an N-terminal RFP (red fluorescent protein) or BFP (blue fluorescent protein) tag. For complementary expression in *S. flexneri*, *icsB* was cloned into the pME6032 vector under the control of a *tac* promoter. For expression in yeast, *icsB* and *ipgA* were cloned into the p414 and p413-Gal vector, respectively, and protein expression was induced by galactose in the media. eGFP-tagged 13 C-terminal residues of RhoA were generated using a standard PCR cloning strategy. RhoA was cloned into pET21a with an N-terminal Flag-6× His tandem tag for recombinant bacterial expression. Complementary DNAs for the α and β subunits of human FTase were amplified from the pRSF-FTase α/β plasmid[48] and constructed into the pACYCDuet vector with an N-terminal 6× His-SUMO tag and an Ulp1 protease digestion site in the FTase α subunit. 24× SunTag and single-chain variable fragment (scFV)-SunTag-eGFP sequences were synthesized at our gene synthesis facility and cloned into the pME6032 and FUIPW vectors, respectively. Point mutations were generated by QuickChange Site-Directed Mutagenesis. All plasmids were verified by DNA sequencing.

Antibodies for CHMP5 (F-7; sc-374338), RhoA (sc-418), eGFP (sc-8334), HA (Y-11; sc-805) and Erk2 (C-14; sc-154) were purchased from Santa Cruz Biotechnology. Antibodies for Myc (9E10) were from Covance. Anti-Flag M2 mouse monoclonal antibody (F4049) and anti-Flag rabbit polyclonal antibody (F7425) were from Sigma–Aldrich. Anti-pan cadherin antibody (ab6529) was from Abcam. Streptavidin-biotinylated horseradish peroxidase complex was from GE Healthcare. All the yeast culture and transformation reagents were from BD Biosciences. Cell culture reagents were Invitrogen products. All other chemicals and reagents used were Sigma–Aldrich products unless otherwise noted.

Yeast, cell culture, bacterial strains and infection.

Culture and transformation of the *S. cerevisiae* W303a strain and assays of IcsB toxicity in yeast cells were performed as described recently[49]. Expression of IcsB and IpgA proteins was induced using 2% galactose as the carbon source in the medium. 293T and HeLa cells were obtained from the American Type Culture Collection. All cell lines were tested to be mycoplasma-free by PCR analyses. The identity of the cells was frequently checked by assessing their morphological features, but has not been authenticated by the short tandem repeat profiling. 293T and HeLa cells were maintained in DMEM supplemented with 10% foetal bovine serum (FBS) and 2 mM L-glutamine at 37 °C in a humidified 5% CO_2 incubator. Transient transfection was performed using the VigoFect (Vigorus) or jetPRIME (Polyplus) reagents following the manufacturers' instructions.

S. flexneri 2a strain 2457T was used in this study. Afimbrial adhesin was transformed into *S. flexneri* to facilitate the infection. Δ*icsB*, Δ*virA* and Δ*virA*Δ*icsB* mutant strains were constructed using the suicide vector pCVD442. For bacterial infection, *S. flexneri* 2457T, *S. typhimurium* SL1344 and *Y. pseudotuberculosis* IP2666 (ΔHEMOJ(T)) were cultured overnight at 37 °C in 2× YT broth with shaking. Before infection, bacteria cultures were diluted by 1:100 in fresh 2× YT broth, and incubated in a shaker until the absorbance at a wavelength of 600 nm reached 1.5. *L. monocytogenes* EGD strain was cultured overnight at 30 °C in brain heart infusion broth with shaking until the absorbance at a wavelength of 600 nm reached 1.5. For fluorescence microscopy, HeLa cells were seeded on glass coverslips in 24-well plates and cultured for 16 h before infections with the indicated multiplicity of infection (MOI) values. The infection was facilitated by centrifugation at 800*g* for 5 min at room temperature followed by another hour of incubation at 37 °C in a 5% CO_2 incubator. Cells were subsequently washed three times with phosphate-buffered saline (PBS) and fresh DMEM containing 100 μg ml^{-1} gentamycin (to kill extracellular bacteria). After another 2 h of incubation, infected cells were washed three times with PBS, then subjected to immunofluorescence staining. Cells cultured on the coverslips were fixed with 4% paraformaldehyde for 30 min at room temperature, permeabilized with 0.1% Triton X-100, blocked with bovine serum albumin or FBS, then incubated with the primary antibody for one hour and the secondary antibody for another hour. Rhodamine-labelled phalloidin was used to stain the F-actin structures.

Plaque formation assay.

HeLa cells were seeded onto 6-well plates and cultured for 24 h before the infection (MOI = 0.05). Bacteria were cultured at 37 °C in 2× YT broth containing 100 μg ml^{-1} streptomycin with shaking at 250 r.p.m. until the absorbance at a wavelength of 600 nm reached 2.0. The infection was facilitated by centrifugation at 800*g* for 5 min at room temperature, and proceeded for 1.5 h at 37 °C in a 5% CO_2 incubator. Cells were subsequently washed with PBS and incubated in 2 ml fresh DMEM containing 10% FBS, 2 mM L-glutamine, 100 μg ml^{-1} gentamycin and 0.5% (w/v) agarose. For *S. flexneri* Δ*virA*Δ*icsB* harbouring pME6032-*icsB*-Flag or other catalytically inactive mutants, bacteria were cultured at 37 °C in 2× YT broth containing 100 μg ml^{-1} streptomycin, 25 μg ml^{-1} tetracycline and 200 μM isopropyl β-D-1-thiogalactopyranoside (IPTG). The infected cells were incubated in fresh DMEM containing 10% FBS, 2 mM l-glutamine, 100 μg ml^{-1} gentamycin, 100 μM IPTG and 0.5%

(w/v) agarose. Afimbrial adhesin transformed into *S. flexneri* was not recommended for this assay. The plaque area (A) was defined as $A=\pi(d/2)^2$, where d was obtained by measuring the diameter (d) of a plaque. The average plaque area was calculated by analysing at least 15 plaques per group.

Protein expression and purification.

Recombinant expression in *E. coli* BL21 cells was induced by 0.4 mM IPTG overnight at 25 °C unless otherwise noted. Expression and purification of GST-RBD and GST (glutathione *S*-transferase)-PBD proteins were previously described[50]. GST-tagged proteins were purified by Glutathione Sepharose resin (GE Healthcare). 6× His tag-fused proteins were purified by Ni-NTA resin (Qiagen). MBP-tagged proteins were purified by the amylose resin (NEB). The proteins were further purified by ion exchange chromatography followed by gel filtration chromatography. All the proteins were concentrated and stored at −20 °C with 20% glycerol in the final volume. The protein concentration was determined by Coomassie blue staining of SDS-PAGE gels using bovine serum albumin standards.

Immunoprecipitation, GST pulldown and western blot analysis.

For immunoprecipitation, approximately 1×10^7 cells were collected 24 h after transfection, and lysed in 1 ml of cell lysis buffer (50 mM Tris-HCl, pH 7.4, 150 mM NaCl, 1 mM EDTA and 0.5% Triton X-100) supplemented with protease inhibitor cocktail (Roche) for 15 min on ice. The cell lysates were centrifuged at 13,000 r.p.m. for 15 min to collect the supernatants. Then, 20 μl of Anti-Flag M2 agarose affinity gel (F2426; Sigma) was added to the supernatants. After 2 h rotation at 4 °C, the beads were washed three times with the cell lysis buffer. For GST pulldown assay, cell lysates were incubated with about 30 μg of GST-RBD/PBD/GDI proteins pre-bound on the glutathione beads. After 1 h rotation at 4 °C, the GST beads were collected and washed three times with the cell lysis buffer. Protein bound on the beads was eluted by boiling in 1× sodium dodecyl sulfate (SDS) sample buffer or by adding 300 ng μl^{-1} Flag peptides to the lysis buffer before immunoblotting analysis, as indicated.

YopT cleavage and Triton X-114 partition assay.

Indicated cells were lysed in an ice-cold buffer containing 50 mM HEPES (pH 7.4), 150 mM NaCl, 1 mM dithiothreitol (DTT) and 1% Triton X-114 supplemented with the protease inhibitor cocktail. Then, 20 μl of clear lysates were incubated with 2 μg of recombinant GST-YopT protein[18] at 30 °C for 1 h. The total lysates were then centrifuged at 13,000 r.p.m. for 10 min and partitioned into the aqueous phase and detergent phase followed by immunoblotting analysis as indicated. For the reconstitution assay, the reactions were supplemented with 1% Triton X-114 (final concentration) and treated with GST-YopT for 1 h before performing the phase partition assay.

In vitro acyltransferase assay.

To prepare the prenylated substrates, equal molar amounts of human FTase complex and Flag-6× His-RhoA or SUMO-RhoA C-terminal 13-residue tail proteins (L193S version) were mixed in a reaction buffer containing 25 mM HEPES (pH 7.4), 20 μM farnesyl

pyrophosphate, 5 mM $MgCl_2$, 5 μM $ZnCl_2$ and 2 mM DTT. The reactions were carried out at 30 °C for 3 h, then loaded onto a HiTrap Q column (GE Healthcare) to collect farnesylated substrate or FTase complex. The farnesylation modification was confirmed by matrixassisted laser desorption/ionization mass spectrometry analysis. To assay the fatty acyltransferase activity of IcsB, 4 μg of farnesylated substrates was incubated with 2 μg of purified IcsB protein in the presence of 0.5 μCi of ^{3}H-stearoyl coenzyme A (Moravek Biochemicals) at 30 °C for 1 h in the reaction buffer containing 40 mM HEPES (pH 7.4), 50 mM NaCl, 1 mM $MgCl_2$, 10 μM $ZnCl_2$, 0.5 mM DTT and 10 μM IP_6. The reactions were stopped by adding 5× SDS sample buffer. Protein samples were separated on 15% SDS-PAGE gel and transferred onto polyvinylidene difluoride membrane followed by Coomassie blue staining. Incorporation of the ^{3}H-stearoyl group was visualized by ^{3}H autoradiography.

Mass spectrometry analyses of RhoA modification by IcsB.

To prepare RhoA samples for total molecular weight measurement by mass spectrometry, 293T cells cultured in 15 cm dishes were transfected with 3× Flag-RhoA Q63L alone or co-transfected with IcsB. Transfected cells were harvested and resuspended in ice-cold buffer containing 25 mM HEPES (pH 7.4), 150 mM NaCl, 1% octyl β-glucopyranoside and the protease inhibitor cocktail. The collected cells were lysed by sonication, and the soluble cleared lysates were incubated with anti-Flag M2 beads for 4 h. The beads were washed extensively with the buffer containing 25 mM HEPES (pH 7.4), 500 mM NaCl and 1% octyl β-glucopyranoside. The bound proteins were eluted by 300 ng μl^{-1} Flag peptide in the elution buffer containing 25 mM HEPES (pH 7.4), 150 mM NaCl and 0.1% octyl β-glucopyranoside. For mass spectrometry, the eluted RhoA protein was loaded onto a homemade capillary column (75 μm inner diameter; 6 cm long) packed with POROS R1 medium (Applied Biosystems). Subsequently, the proteins were eluted by an Agilent 1100 binary pump system with the following gradient: 0–80% B in 30 min (A = 0.1 M acetic acid in water; B = 0.1 M acetic acid in 80% acetonitrile/water), then sprayed into a QSTAR XL mass spectrometer (AB Sciex) equipped with a Nano Electrospray ion source. The instrument was acquired in MS mode under 2,100 volts of spray voltage. The protein charge envelope was averaged across the corresponding protein elution peaks and deconvoluted into the uncharged form using the BioAnalyst software provided by the manufacturer. To identify the exact lipid modification, the above purified RhoA was subjected to trypsin digestion as described previously[51]. The resulting peptides were separated on an EASY-nLC 1000 system (Thermo Fisher Scientific). Peptides eluted from the capillary column were applied directly onto a hybrid LTQ-Orbitrap Elite mass spectrometer by electrospray (Thermo Fisher Scientific) for mass spectrometry (MS) and MS/MS analyses.

In-gel fluorescence assay.

293T cells grown at the confluency of 60–70% in 10 cm dishes were co-transfected with Flag-tagged IcsB substrates and IcsB-WT or IcsB C306A. Some 4 h after transfection, the media were replaced with fresh media containing 50 μM Alk-16. To examine substrate modification during infection, 293T transfected with Flag-tagged IcsB substrates for 24 h were infected with the indicated *S. flexneri* strains (MOI = 100) in the presence of 50 μM Alk-16. Some 28 h after the co-transfection, or 2 h after the infection, the cells were harvested and the substrates were subjected to anti-Flag immunoprecipitation. The

immunoprecipitates were washed once with the cell lysis buffer (50 mM Tris-HCl, pH 7.4, 150 mM NaCl, 1 mM EDTA and 0.5% Triton X-100) and another three times with the wash buffer (50 mM Tris-HCl, pH 7.4, 150 mM NaCl). In-gel click reactions with 100 μM azido-rhodamine in the buffer containing 25 mM HEPES (pH 7.4), 1 mM $CuSO_4$, 1 mM TCEP, 100 μM TBTA and 150 mM NaCl were then performed (4 h, room temperature). The samples were then heated at 95 °C for 20 min in the presence of freshly prepared NH_2OH (0.75 M) before being loaded onto 4−20% Tris-HCl gels (Bio-Rad) for SDS-PAGE separation. Gels were scanned on the Bio-Rad ChemiDoc Imaging System.

Chemical proteomic profiling of IcsB-modified proteins.

HeLa cells were grown in DMEM supplemented with 4.5 gl^{-1} D-glucose, 110 mg l^{-1} sodium pyruvate and 10% FBS (HyClone; Thermo Fisher Scientific). For the SILAC experiments, cells were cultured in arginine- and lysine-deficient DMEM (Thermo Fisher Scientific) supplemented with 10% dialysed FBS. For the culture of ‘light’-labelled cells, SILAC medium containing $^{12}C_6$-L-lysine-2HCl (Lys0; 0.80 mM; Sigma) and $^{12}C_6$-l-arginine-HCl (Arg0; 0.40 mM; Sigma) was used. For the culture of ‘heavy’labelled cells, SILAC medium containing $^{13}C_6$,$^{15}N_2$-L-lysine-2HCl (Lys8; 0.80 mM; Cambridge Isotope) and $^{13}C_6$,$^{15}N_4$-L-arginine-HCl (Arg10; 0.40 mM; Cambridge Isotope) was used. After seven cell doublings, the incorporation of the heavy isotopes was estimated to be > 98% as determined by liquid chromatography MS/MS (LC-MS/MS) analysis.

HeLa cells were transfected with the indicated eGFP-IcsB plasmid for 6 h and labelled with DMSO or Alk-16 (25 μM) overnight. Alternatively, HeLa cells labelled with Alk-16 (50 μM) for 1 h were infected with *S. flexneri* WT or Δ *icsB* for 1.5 h. The media were then replaced with fresh media containing 100 μg ml^{-1} gentamicin and 50 μM Alk-16. Infected cells were further incubated for 1 h, then washed with PBS twice. For both assays, cells were lysed with 4% SDS (50 mM triethanolamine with 150 mM NaCl, pH 7.4) with vigorous vortexing and sonication. The cell lysates were centrifuged at 16,000*g* for 20 min at room temperature to remove cellular debris. Protein concentrations were determined using the BCA assay (Pierce). For in-gel fluorescence visualization, whole cell lysates (50 μg) diluted with SDS lysis buffer (1 mg ml^{-1}) were reacted with a freshly prepared click-chemistry reaction cocktail containing azido-rhodamine, TCEP, TBTA and $CuSO_4$ for 1 h at room temperature[30]. The reactions were terminated by the addition of ice-cold methanol (1 ml). The mixtures were placed at −20 °C overnight, then centrifuged at 18,000*g* for 20 min at 4 °C. The protein pellets were washed with ice-cold MeOH twice, air-dried for 10 min, resuspended in 35 μl of SDS lysis buffer, and then diluted with 12.5 μl of 4× reducing SDS sample buffer and 2.5 μl of 2-mercaptoethanol. The samples were heated for 5 min at 95 °C in the presence of freshly prepared NH_2OH (0.75 M) before being loaded onto 4−20% Tris-HCl gels (Bio-Rad) for SDS-PAGE separation. Gels were de-stained in 40% methanol and 10% acetic acid for at least 1 h, then scanned on a GE Healthcare Typhoon 9400 variable mode imager with excitation and emission at 532 and 580 nm, respectively. The gels were then also stained with Coomassie Brilliant Blue (Bio-Rad).

For the SILAC proteomics studies, ‘heavy’- and ‘light’-labelled cells were transfected with eGFP-tagged WT or the C306A mutant IcsB in the ‘forward’ experiment and vice versa in

the ‘reverse’ experiment. For the infection assay, ‘heavy’- and ‘light’-labelled cells were infected with *S. flexneri* WT or Δ*icsB* strain in the ‘forward’ experiment and vice versa in the ‘reverse’ experiment. Cells were labelled with Alk-16 and lysed with 4% SDS as described above. After estimating the protein concentration, ‘heavy’-labelled cell lysates (1 mg) were mixed with ‘light’-labelled cell lysates (1 mg) and treated with freshly prepared NH_2OH (0.75 M) at room temperature with rotation for 1 h. Proteins were then precipitated with ice-cold MeOH, resuspended in 4% SDS and clicked with azido-biotin using CuAAC reactions as above described. Methanol-precipitated and washed protein pellets were again resuspended in 4% SDS. Equal amounts of each protein were diluted 1/4 by volume with 50 mM triethanolamine buffer (final 1% SDS). Then, 60 μl of prewashed streptavidin agarose beads (Invitrogen) were added to each sample. The protein and bead mixtures were incubated for 1 h at room temperature on a nutating mixer. The beads were then washed once with PBS containing 0.2% (w/v) SDS, three times with PBS and twice with 250 mM ammonium bicarbonate. Beads were resuspended in 500 μl of 8 M urea, reduced with 10 mM DTT for 30 min, then alkylated with 50 mM iodoacetamide in the dark for another 30 min. Finally, the beads were washed with 25 mM ammonium bicarbonate and digested with 0.5 μg of trypsin at 37 °C overnight. The supernatants were collected, dried and pre-fractionated with SCX StageTips for LC-MS analysis.

LC-MS/MS analysis for proteomic profiling was carried out at the Proteomics Resource Center at The Rockefeller University, New York, NY, USA. LC-MS analysis was performed with a Dionex 3000 nano-HPLC coupled to an Orbitrap XL mass spectrometer (Thermo Fisher Scientific). Peptide samples were loaded onto a C18 reverse-phase column (75 μm diameter, 15 cm length). A 180 min gradient increasing from 95% buffer A (water with 0.1% formic acid) and 5% buffer B (acetonitrile with 0.1% formic acid) to 75% buffer B in 133 min was used at 0.2 μl min^{-1} to inject the samples into the mass spectrometer. The Orbitrap XL was operated in top-8-CID-mode with MS spectra measured at a resolution of 60,000 FWHM (full width at half maximum) at m/z = 400. One full MS scan (300–2,000 molecular weight) was followed by three data-dependent scans of the tth nth most intense ions with dynamic exclusion enabled. Peptides fulfilling a Percolator-calculated 1% false discovery rate threshold were reported. Acquired tandem MS spectra were extracted and quantified using MaxQuant software[52]. The search results from MaxQuant were analysed by Perseus (http://www.perseus-framework.org). Enzyme specificity was set to trypsin, allowing two missed cleavages. Carbamidomethylation of cysteine was set as a fixed modification, while methionine oxidation and N-terminal acetylation were set as variable modifications. Mass deviation for MS/MS peaks was set at a maximum of 0.5 m/z units, and maximum false discovery rates were set to 0.01, both at the peptide and the protein levels. Peak lists generated by MaxQuant were searched with Andromeda against the UniProt complete human database concatenated with common known contaminants. Only unique and razor peptides were used for quantification with a minimum of two ratio counts. The ‘re-quantify’ feature of MaxQuant was used to correct the quantification of proteins with high ratios. Before analysis, known contaminants and reverse hits were removed.

In this study, no statistical methods were used to predetermine the sample size. The experiments were not randomized, and the investigators were not blinded to allocation during the experiments and outcome assessment.

Supplementary Material

Refer to Web version on PubMed Central for supplementary material.

Acknowledgements

We thank R. Isberg for providing *Yersinia* strains, G. Praefcke for the pRSF-FTase plasmid, and the Proteomics Resource Center at The Rockefeller University for mass spectrometry analysis. We also thank members of the Shao laboratory for technical assistance and stimulating discussions. This work was supported by the Basic Science Center Project of the National Natural Science Foundation of China (81788101), National Key Research and Development Program of China (2017YFA0505900 and 2016YFA0501500) and Strategic Priority Research Program of the Chinese Academy of Sciences (XDB08020202) to F.S. H.C.H. acknowledges support from NIH-NIGMS grant R01 GM087544. The research was also supported in part by an International Early Career Scientist grant from the Howard Hughes Medical Institute and Beijing Scholar Program to F.S.

References

1. Cui J & Shao F Biochemistry and cell signaling taught by bacterial effectors. Trends Biochem. Sci 36, 532–540 (2011). [PubMed: 21920760]
2. Carayol N & Tran Van Nhieu G The inside story of Shigella invasion of intestinal epithelial cells. Cold Spring Harb. Perspect. Med 3, a016717 (2013). [PubMed: 24086068]
3. Ashida H, Mimuro H & Sasakawa C *Shigella* manipulates host immune responses by delivering effector proteins with specific roles. Front Immunol. 6, 219 (2015). [PubMed: 25999954]
4. Mellouk N & Enninga J Cytosolic access of intracellular bacterial pathogens: the *Shigella* paradigm. Front. Cell. Infect. Microbiol 6, 35 (2016). [PubMed: 27092296]
5. Li H et al. The phosphothreonine lyase activity of a bacterial type III effector family. Science 315, 1000–1003 (2007). [PubMed: 17303758]
6. Zhu Y et al. Structural insights into the enzymatic mechanism of the pathogenic MAPK phosphothreonine lyase. Mol. Cell 28, 899–913 (2007). [PubMed: 18060821]
7. Mazurkiewicz P et al. SpvC is a *Salmonella* effector with phosphothreonine lyase activity on host mitogen-activated protein kinases. Mol. Microbiol 67, 1371–1383 (2008). [PubMed: 18284579]
8. Goto Y et al. Discovery of unique lanthionine synthetases reveals new mechanistic and evolutionary insights. PLoS Biol. 8, e1000339 (2010). [PubMed: 20351769]
9. Allaoui A, Mounier J, Prevost MC, Sansonetti PJ & Parsot C *icsB*: a *Shigella flexneri* virulence gene necessary for the lysis of protrusions during intercellular spread. Mol. Microbiol 6, 1605–1616 (1992). [PubMed: 1495389]
10. Ogawa M, Suzuki T, Tatsuno I, Abe H & Sasakawa C IcsB, secreted via the type III secretion system, is chaperoned by IpgA and required at the post-invasion stage of *Shigella* pathogenicity. Mol. Microbiol 48, 913–931 (2003). [PubMed: 12753186]
11. Ogawa M et al. Escape of intracellular *Shigella* from autophagy. Science 307, 727–731 (2005). [PubMed: 15576571]
12. Kayath CA et al. Escape of intracellular *Shigella* from autophagy requires binding to cholesterol through the type III effector, IcsB. Microbes Infect 12, 956–966 (2010). [PubMed: 20599519]
13. Baxt LA & Goldberg MB Host and bacterial proteins that repress recruitment of LC3 to Shigella early during infection. PLoS ONE 9, e94653 (2014). [PubMed: 24722587]
14. Mostowy S et al. Entrapment of intracytosolic bacteria by septin cage-like structures. Cell Host Microbe 8, 433–444 (2010). [PubMed: 21075354]
15. Campbell-Valois FX, Sachse M, Sansonetti PJ & Parsot C Escape of actively secreting Shigella flexneri from ATG8/LC3-positive vacuoles formed during cell-to-cell spread is facilitated by IcsB and VirA. mBio 6, e02567–14 (2015). [PubMed: 26015503]
16. Pei J & Grishin NV The Rho GTPase inactivation domain in *Vibrio cholerae* MARTX toxin has a circularly permuted papain-like thiol protease fold. Proteins 77, 413–419 (2009). [PubMed: 19434753]

17. Ahrens S, Geissler B & Satchell KJ Identification of a His–Asp–Cys catalytic triad essential for function of the Rho inactivation domain (RID) of Vibrio cholerae MARTX toxin. J. Biol. Chem 288, 1397–1408 (2013). [PubMed: 23184949]
18. Shao F, Merritt PM, Bao Z, Innes RW & Dixon JE A *Yersinia* effector and a *Pseudomonas* avirulence protein define a family of cysteine proteases functioning in bacterial pathogenesis. Cell 109, 575–588 (2002). [PubMed: 12062101]
19. Sheahan KL & Satchell KJ Inactivation of small Rho GTPases by the multifunctional RTX toxin from *Vibrio cholerae*. Cell. Microbiol 9, 1324–1335 (2007). [PubMed: 17474905]
20. Lemichez E & Aktories K Hijacking of Rho GTPases during bacterial infection. Exp. Cell Res 319, 2329–2336 (2013). [PubMed: 23648569]
21. Shao F et al. Biochemical characterization of the *Yersinia* YopT protease: cleavage site and recognition elements in Rho GTPases. Proc. Natl Acad. Sci. USA 100, 904–909 (2003). [PubMed: 12538863]
22. Hoffman GR, Nassar N & Cerione RA Structure of the Rho family GTP-binding protein Cdc42 in complex with the multifunctional regulator RhoGDI. Cell 100, 345–356 (2000). [PubMed: 10676816]
23. Mukherjee S et al. *Yersinia* YopJ acetylates and inhibits kinase activation by blocking phosphorylation. Science 312, 1211–1214 (2006). [PubMed: 16728640]
24. Lupardus PJ, Shen A, Bogyo M & Garcia KC Small molecule-induced allosteric activation of the *Vibrio cholerae* RTX cysteine protease domain. Science 322, 265–268 (2008). [PubMed: 18845756]
25. Prochazkova K & Satchell KJ Structure–function analysis of inositol hexakisphosphate-induced autoprocessing of the *Vibrio cholerae* multifunctional autoprocessing RTX toxin. J. Biol. Chem 283, 23656–23664 (2008). [PubMed: 18591243]
26. Calder T et al. Vibrio type III effector VPA1380 is related to the cysteine protease domain of large bacterial toxins. PLoS ONE 9, e104387 (2014). [PubMed: 25099122]
27. Mittal R, Peak-Chew SY, Sade RS, Vallis Y & McMahon HT The acetyltransferase activity of the bacterial toxin YopJ of *Yersinia* is activated by eukaryotic host cell inositol hexakisphosphate. J. Biol. Chem 285, 19927–19934 (2010). [PubMed: 20430892]
28. Hang HC & Linder ME Exploring protein lipidation with chemical biology. Chem. Rev 111, 6341–6358 (2011). [PubMed: 21919527]
29. Grammel M & Hang HC Identification of lysine acetyltransferase substrates using bioorthogonal chemical proteomics. Methods Mol. Biol 981, 201–210 (2013). [PubMed: 23381864]
30. Charron G et al. Robust fluorescent detection of protein fatty-acylation with chemical reporters. J. Am. Chem. Soc 131, 4967–4975 (2009). [PubMed: 19281244]
31. Wilson JP, Raghavan AS, Yang YY, Charron G & Hang HC Proteomic analysis of fatty-acylated proteins in mammalian cells with chemical reporters reveals *S*-acylation of histone H3 variants. Mol. Cell Proteom 10, M110.001198 (2011).
32. Dong N et al. Structurally distinct bacterial TBC-like GAPs link Arf GTPase to Rab1 inactivation to counteract host defenses. Cell 150, 1029–1041 (2012). [PubMed: 22939626]
33. Tanenbaum ME, Gilbert LA, Qi LS, Weissman JS & Vale RD A protein-tagging system for signal amplification in gene expression and fluorescence imaging. Cell 159, 635–646 (2014). [PubMed: 25307933]
34. Li P et al. Ubiquitination and degradation of GBPs by a *Shigella* effector to suppress host defence. Nature 551, 378–383 (2017). [PubMed: 29144452]
35. Shim JH et al. CHMP5 is essential for late endosome function and down-regulation of receptor signaling during mouse embryogenesis. J. Cell Biol 172, 1045–1056 (2006). [PubMed: 16567502]
36. Ward DM et al. The role of LIP5 and CHMP5 in multivesicular body formation and HIV-1 budding in mammalian cells. J. Biol. Chem 280, 10548–10555 (2005). [PubMed: 15644320]
37. Shibutani ST, Saitoh T, Nowag H, Munz C & Yoshimori T Autophagy and autophagy-related proteins in the immune system. Nat. Immunol 16, 1014–1024 (2015). [PubMed: 26382870]
38. Choy A et al. The *Legionella* effector RavZ inhibits host autophagy through irreversible Atg8 deconjugation. Science 338, 1072–1076 (2012). [PubMed: 23112293]

39. Resh MD Fatty acylation of proteins: the long and the short of it. Prog. Lipid Res 63, 120–131 (2016). [PubMed: 27233110]
40. Hannoush RN Synthetic protein lipidation. Curr. Opin. Chem. Biol 28, 39–46 (2015). [PubMed: 26080277]
41. Nadolski MJ & Linder ME Protein lipidation. FEBS J. 274, 5202–5210 (2007). [PubMed: 17892486]
42. Schey KL, Gutierrez DB, Wang Z, Wei J & Grey AC Novel fatty acid acylation of lens integral membrane protein aquaporin-0. Biochemistry 49, 9858–9865 (2010). [PubMed: 20942504]
43. Stevenson FT, Bursten SL, Fanton C, Locksley RM & Lovett DH The 31-kDa precursor of interleukin 1 alpha is myristoylated on specific lysines within the 16-kDa N-terminal propiece. Proc. Natl Acad. Sci. USA 90, 7245–7249 (1993). [PubMed: 8346241]
44. Jiang H et al. SIRT6 regulates TNF-alpha secretion through hydrolysis of long-chain fatty acyl lysine. Nature 496, 110–113 (2013). [PubMed: 23552949]
45. Zhang X, Spiegelman NA, Nelson OD, Jing H & Lin H SIRT6 regulates Ras-related protein R-Ras2 by lysine defatty-acylation. eLife 6, e25158 (2017). [PubMed: 28406396]
46. Zhou Y et al. N^{ε}-fatty acylation of Rho GTPases by a MARTX toxin effector. Science 358, 528–531 (2017). [PubMed: 29074776]
47. Dolores JS, Agarwal S, Egerer M & Satchell KJ *Vibrio cholerae* MARTX toxin heterologous translocation of beta-lactamase and roles of individual effector domains on cytoskeleton dynamics. Mol. Microbiol 95, 590–604 (2015). [PubMed: 25427654]
48. Fres JM, Muller S & Praefcke GJ Purification of the CaaX-modified, dynamin-related large GTPase hGBP1 by coexpression with farnesyltransferase. J. Lipid Res 51, 2454–2459 (2010). [PubMed: 20348589]
49. Dong N et al. Modulation of membrane phosphoinositide dynamics by the phosphatidylinositide 4-kinase activity of the Legionella LepB effector. Nat. Microbiol 2, 16236 (2016). [PubMed: 27941800]
50. Pellegrin S & Mellor H Rho GTPase activation assays. Curr. Protoc. Cell Biol 38, 14.8.1–14.8.19 (2008).
51. Hu M, Liu Y, Yu K & Liu X Decreasing the amount of trypsin in in-gel digestion leads to diminished chemical noise and improved protein identifications. J. Proteom 109, 16–25 (2014).
52. Cox J & Mann M MaxQuant enables high peptide identification rates, individualized p.p.b.-range mass accuracies and proteome-wide protein quantification. Nat. Biotechnol 26, 1367–1372 (2008). [PubMed: 19029910]

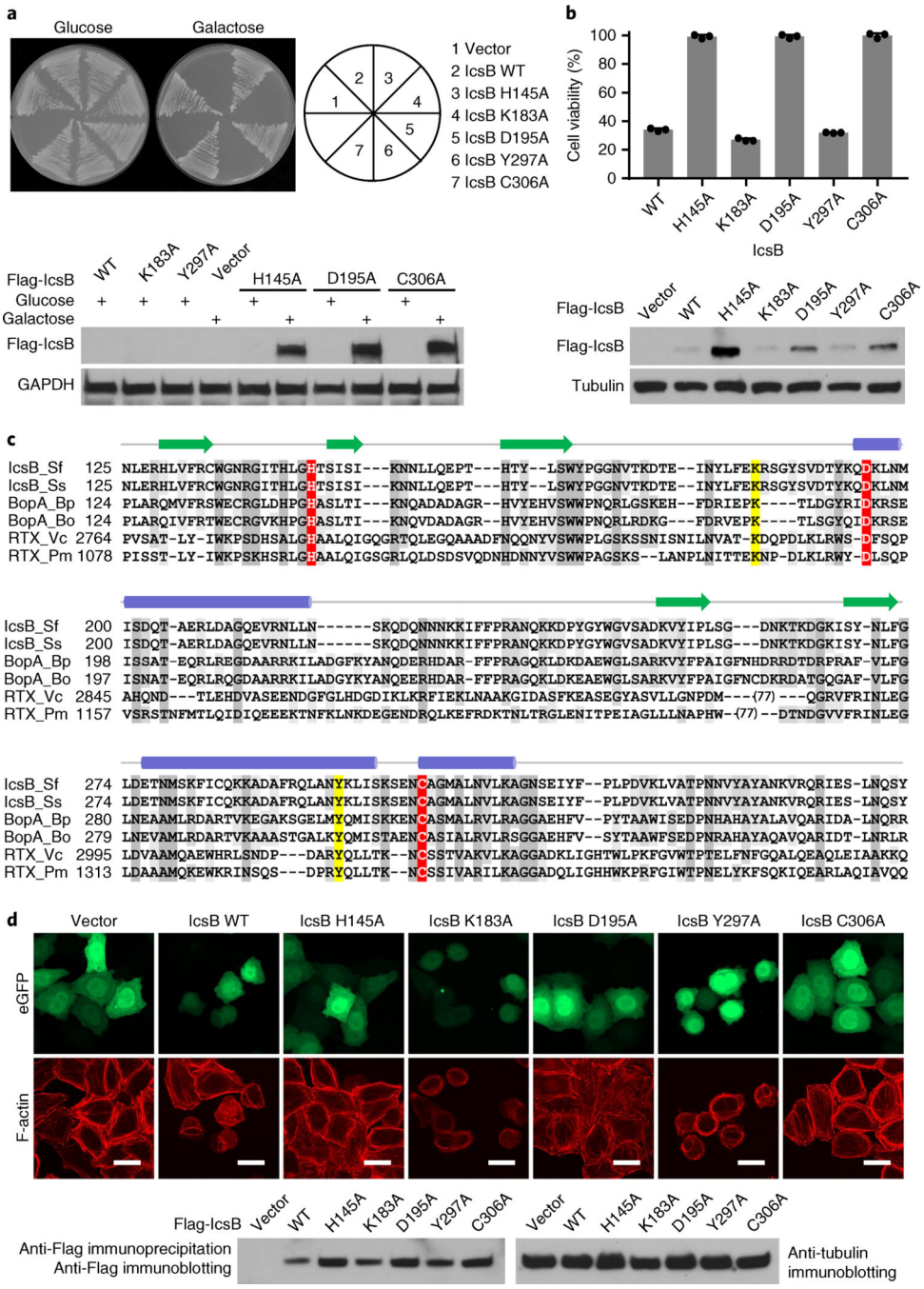

Fig. 1 |. ectopic expression of IcsB is toxic to yeast and disrupts the actin cytoskeleton in mammalian cells, which requires the putative catalytic motif.

a, Effects of IcsB expression on yeast growth. *S. cerevisiae* strains harbouring an empty vector or an indicated galactose-inducible IcsB expression plasmid were stripped onto the selective media containing glucose or galactose. Cells cultured in the liquid media were subjected to western blot analysis (bottom). **b**, Effects of IcsB expression on mammalian cell viability. 293T cells were transfected with an empty vector or an indicated IcsB expression plasmid. Cell viability was determined by measuring cytosolic ATP levels normalized to the

vector control (mean ± s.d. from three replicates). Bottom: immunoblots of IcsB expression. **c**, Sequence alignment of the IcsB family. IcsB_Sf and IcsB_Ss are IcsB of *S. flexneri* and *S. sonnei*, respectively. BopA_Bp and BopA_Bo are BopA of *B. pseudomallei* and *Burkholderia oklahomensis*, respectively. RTX_Vc and RTX_Pm are RIDs of MARTX toxins from *Vibrio cholerae* and *Proteus mirabilis*, respectively. In total, 77 amino acids of RTX_Vc and RTX_Pm that are not conserved were omitted from the alignment. The putative catalytic residues and other conserved residues are coloured in red and grey, respectively. The yellow-coloured residues are not required for cytotoxicity of IcsB in yeast and 293T cells. Secondary structures predicted from IcsB sequence are shown above the sequence. Blue ovals represent α helices and green arrows represent β strands. **d**, Effects of IcsB expression on filamentous actin cytoskeleton structure. HeLa cells were co-transfected with eGFP and an indicated Flag-IcsB expression plasmid. F-actin was stained by rhodamine phalloidin. Scale bars, 20 μm. Total cell lysates were subjected to anti-Flag immunoprecipitation followed by anti-Flag immunoblotting (bottom). The data in **a**, **b** and **d** are representative of three independent experiments.

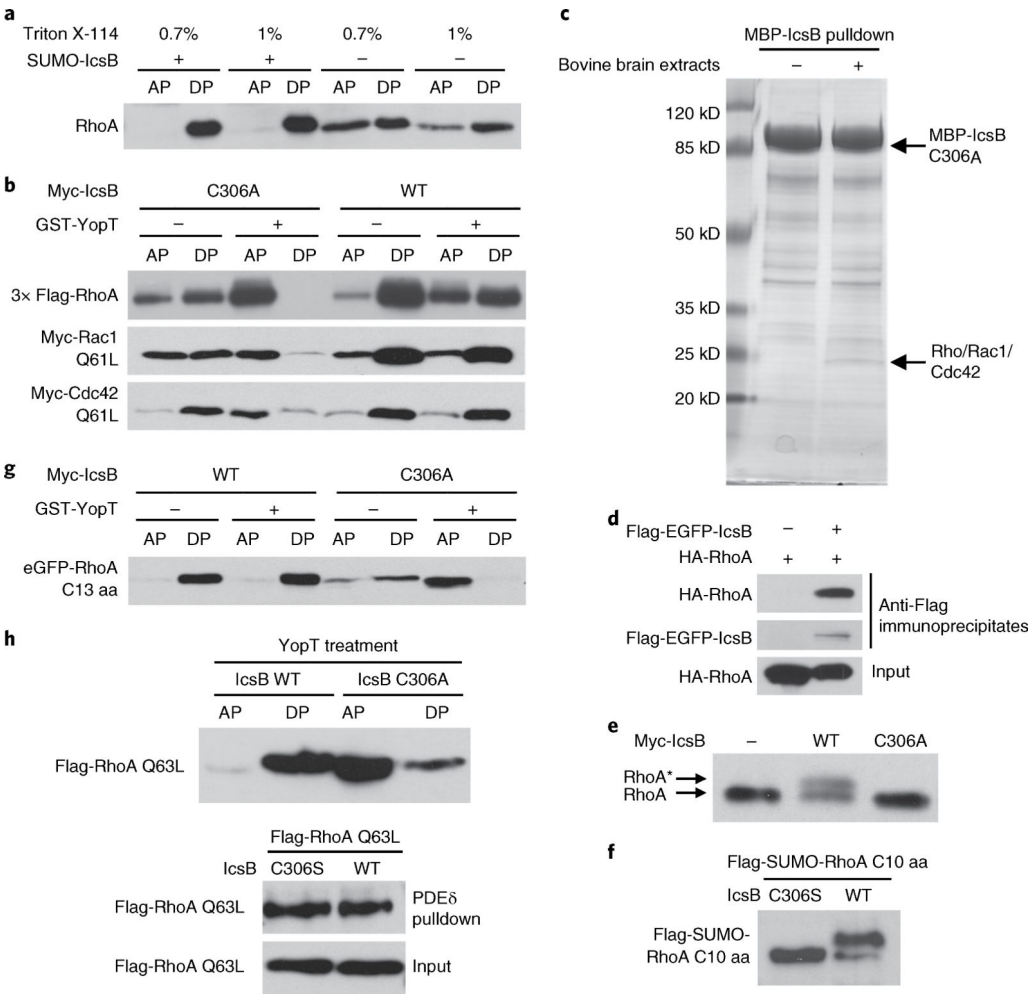

Fig. 2 |. IcsB disrupts RhogTPase membrane cycling by modifying its C-terminal tail.

a, Effects of IcsB on the hydrophobicity of RhoA. Cytosolic extracts of RhoA-transfected 293T cells were incubated with purified IcsB and ATP followed by Triton X-114 partitioning. **b**, Effects of IcsB on RhoGTPase cleavage by YopT. 293T cells were co-transfected with an indicated Rho expression plasmid and IcsB (WT or C306A). Cell lysates were treated with or without YopT, then subjected to Triton X-114 partitioning. **c**, Identification of RhoGTPases as IcsB-binding proteins. Purified MBP-IcsB C306A was incubated with or without bovine brain extracts and then subjected to amylose bead pulldown. Bound proteins were separated on the SDS-PAGE gel and Coomassie blue staining of the gel is shown. The specific band bound by IcsB C306A contains Rho, Rac and Cdc42, revealed by mass spectrometry. **d**, Interaction between transfected IcsB and RhoA in 293T cells. Shown are immunoblots of anti-Flag immunoprecipitates and total cell lysates (input). **e**,**f**, SDS-PAGE mobility shift of the endogenous RhoA or RhoA C-terminal tail induced by IcsB. 293T cells were transfected with an indicated IcsB expression plasmid alone (**e**) or co-transfected with a Flag-SUMO-tagged RhoA C-terminal ten-residue tail (C10 aa) (**f**). Cell lysates were subjected to 15% SDS-PAGE, followed by immunoblotting analyses. The asterisk in (**e**) indicates the mobility shift of the endogenous RhoA. **g**, Effects of IcsB on the cleavage of the RhoA C-terminal tail by YopT. 293T cells were co-transfected

with an eGFP-tagged RhoA C-terminal 13-residue tail (C13 aa) and IcsB (WT or C306A). Cell lysates were treated with or without YopT, then subjected to Triton X-114 partitioning. **h**, Effects of IcsB on RhoA precipitation by PDEδ. 293T cells were co-transfected with Flag-RhoA Q63L and an indicated IcsB expression plasmid. Cell lysates were subjected to GST-PDEδ pulldown or YopT digestion followed by Triton X-114 partitioning. Proteins in the aqueous phase (AP) and detergent phase (DP) were subjected to immunoblotting analyses (**a**, **b**, **g** and **h**). All data (**a**–**h**) are representative of three independent experiments.

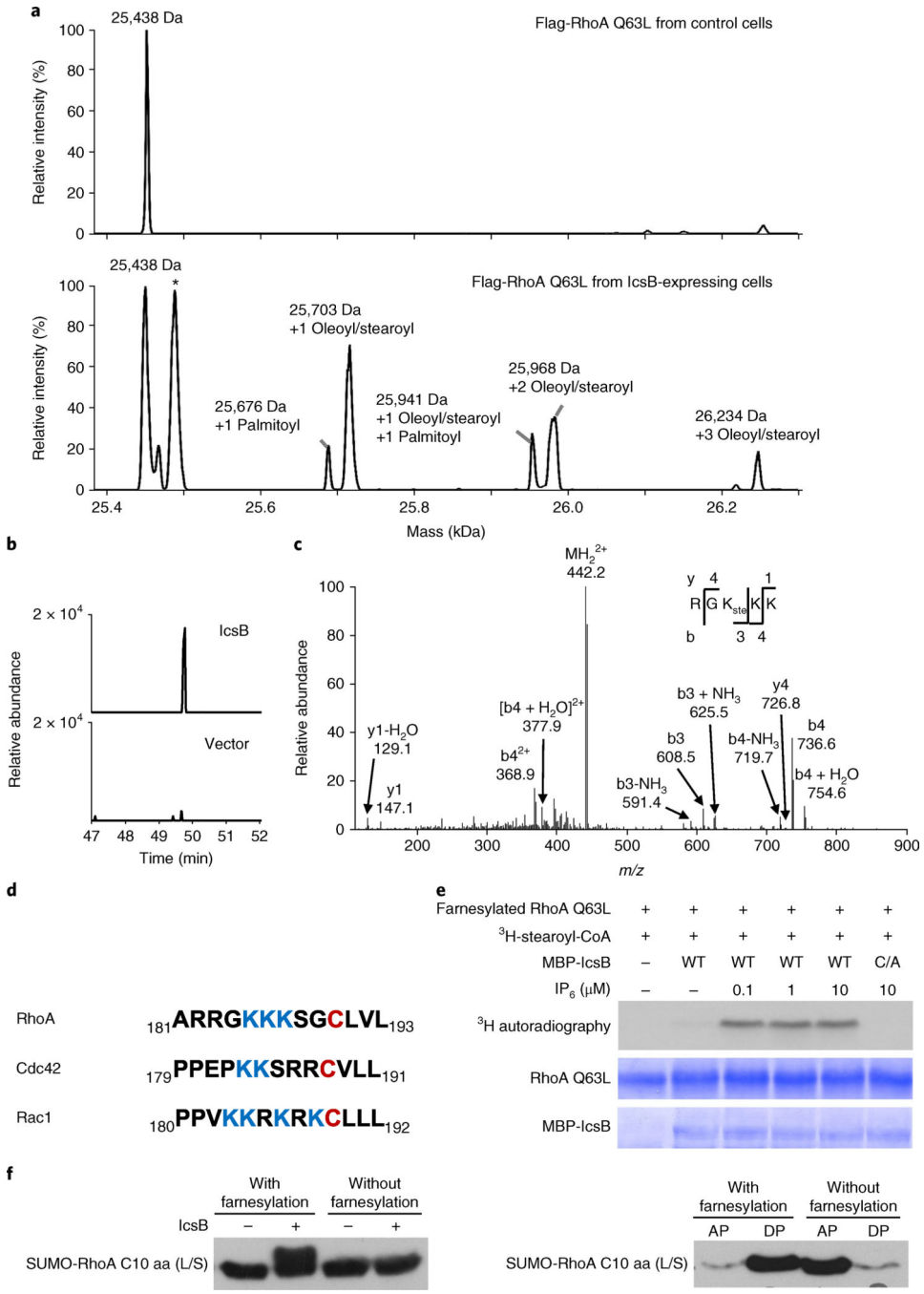

Fig. 3 |. IcsB is an 18-carbon *N*-fatty acyltransferase that modifies lysine residues in the C-terminal PBR of RhogTPases.

a, Mass spectrometry identification RhoA modification by IcsB in transfected 293T cells. Flag-RhoA Q63L was purified using the anti-Flag affinity resin. The total molecular mass was determined by electrospray ionization mass spectrometry. The asterisk denotes RhoA Q63L without the prenylation modification. **b**, Extracted ion chromatograms of Flag-RhoA Q63L purified from transfected 293T cells. Shown are graphs of the stearoylated peptide RGKKK (m/z = 441.8). **c**, MS/MS mass spectrum of the stearoylated peptide RGKKK in

IcsB-modified Flag-RhoA Q63L purified from 293T cells. b and y fragments in (**c**) are obtained from the MS/MS spectra of the fatty acylated peptide (RGK(ste)KK)**. d**, Alignment of the RhoA, Cdc42 and Rac1 C-terminal 13-residue sequences. The prenylated cysteine residues are in red, and the PBR lysines are in blue. **e**, In vitro reconstitution of RhoA stearoylation by IcsB. Purified farnesylated RhoA was incubated with MBP-IcsB, ^{3}H-stearoyl-CoA and the indicated concentration of IP_6. The reactions were stopped by adding the SDS sample buffer, and subjected to SDS-PAGE followed by Coomassie blue staining and ^{3}H autoradiography. **f**, Requirement of RhoA prenylation for fatty acylation by IcsB. The farnesylated or unmodified Flag-SUMO-RhoA C-terminal 10-residue (C10 aa) tail was incubated with SUMO-IcsB, ATP and cell extracts. The reactions were stopped by adding the SDS sample buffer, then subjected to 15% SDS-PAGE followed by anti-Flag immunoblotting (left). Cell lysates were also subjected to Triton X-114 partitioning (AP, aqueous phase; DP, detergent phase; right). L/S is an L193S mutation that switches the native geranylgeranylation to farnesylation. Data in **a**–**c**, **e** and **f** are representative of three independent experiments.

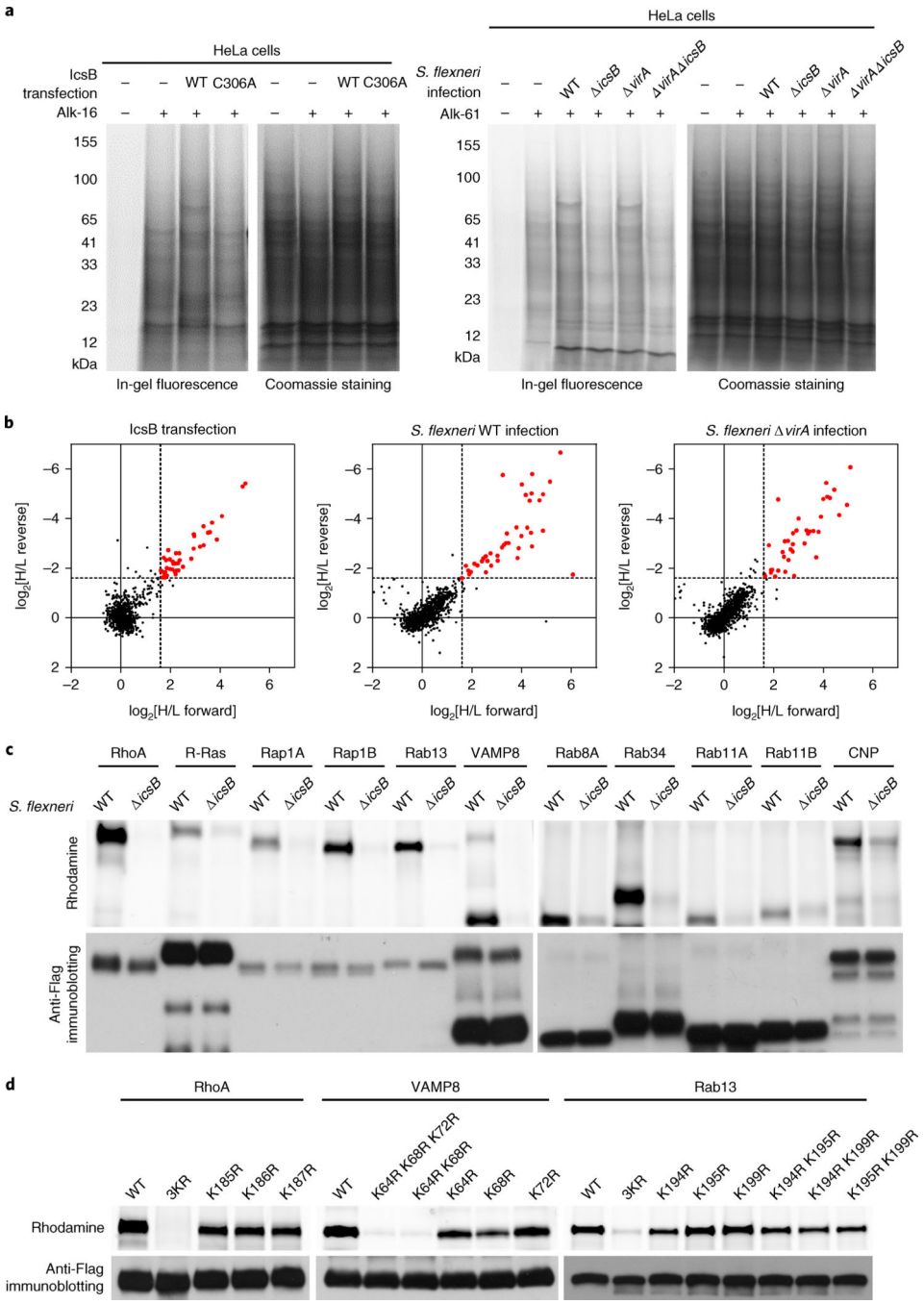

Fig. 4 |. Chemical proteomics reveals that IcsB targets multiple host membrane proteins for lysine N^{ε}-fatty acylation.

a, In-gel fluorescence visualization of the stearoylome profile of IcsB (WT or C306A)-transfected (left) and *S. flexneri* (WT, Δ*icsB*, Δ *virA* or Δ *virA*Δ *icsB*)-infected (right) HeLa cells. Coomassie blue staining confirms equal protein loading. **b**, Scatter plots of SILAC proteomic data. Hits with an abundance increase of more than threefold ($\log_2$[H/L > 1.58] in the forward SILAC and $\log_2$[H/L < − 1.58] in the reverse SILAC) in the IcsB group relative to the control group are shown in red. H/L represents the ratio between heavy and light label

partners in the indicated (forward or reverse) experiment. **c**, Validation of IcsB modification of the proteomic hits. A total of 11 selected candidate substrates were individually transfected into 293T cells. The cells were infected with *S. flexneri* WT or Δ*icsB* in the presence of Alk-16, and subjected to in-gel fluorescence assay. Anti-Flag immunoblotting confirms equal loading of the indicated samples. **d**, Effects of lysine mutation in the PBR of selected substrates on their modification by IcsB. 293T cells were co-transfected with IcsB and Flag-tagged RhoA, VAMP8 or Rab13, or the indicated lysine mutant. The cells were metabolized with Alk-16 and subjected to in-gel fluorescence assay. Data are representative of two (**a** and **b**) or three (**c** and **d**) independent experiments.

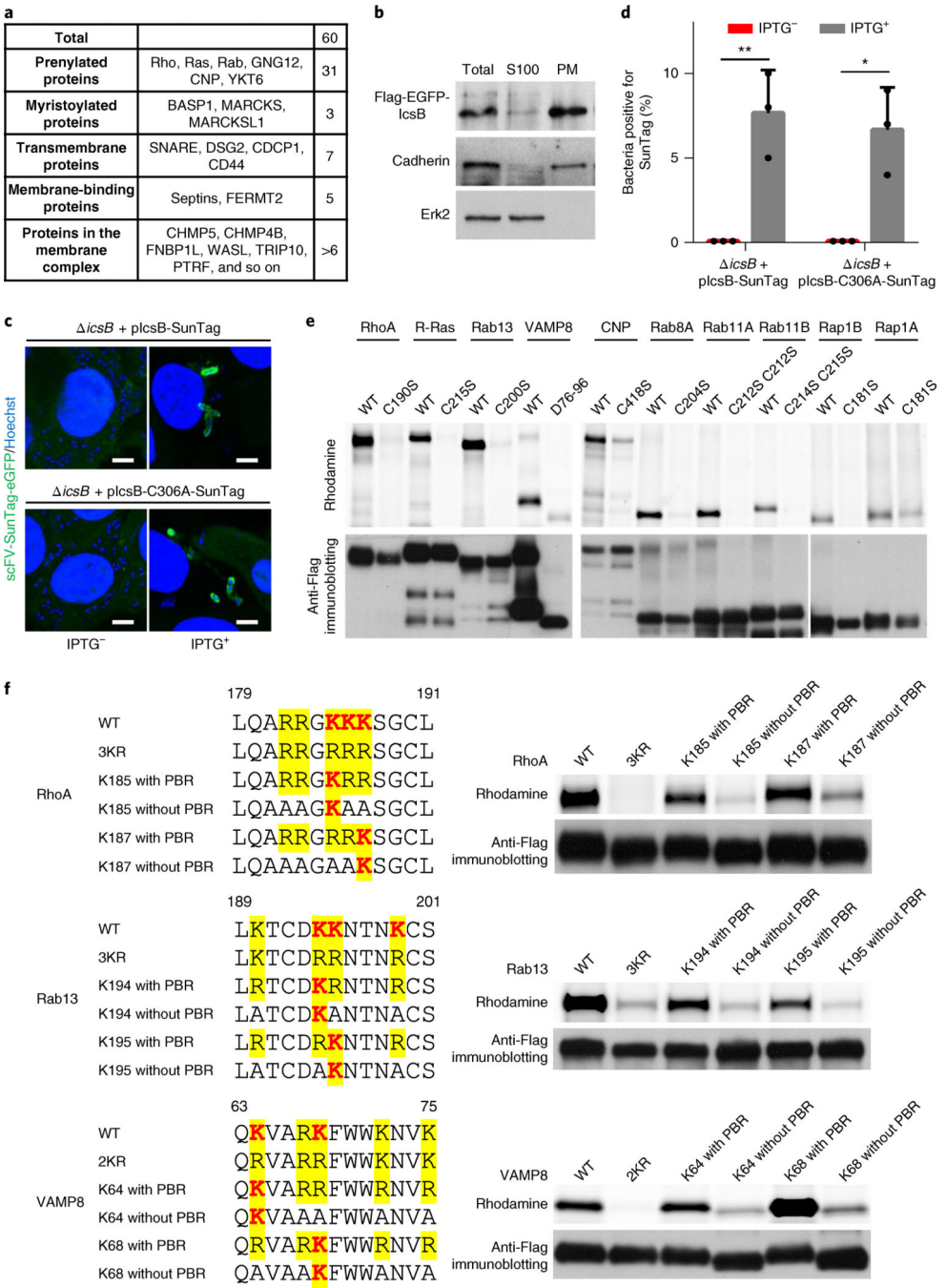

Fig. 5 |. IcsB is localized on *Shigella*-containing vacuoles and modifies its substrates on the membrane location.

a, Classification of IcsB substrates by their membrane-targeting mechanisms. **b**, Sub-cellular fractionation of IcsB. 293T cells transfected with Flag-eGFP-IcsB were lysed in hypotonic buffer, and the cell lysates (S10) were ultracentrifuged (100,000*g*) to obtain the plasma membrane (PM) and the S100 cytoplasmic fraction. Shown are the anti-Flag, anti-cadherin and anti-Erk2 immunoblots. **c**,**d**, Localization of IcsB during *S. flexneri* infection. HeLa cells stably expressing scFV-SunTag-eGFP were infected with *S. flexneri* Δ *icsB*

complemented with 24× SunTag-fused IcsB (WT or C306A). IPTG was used to induce IcsB expression. Fluorescence images taken at 4 h post-infection are shown in **c** (scale bars, 3 μm), and percentages of intracellular bacteria containing SunTag-positive signals are shown in **d**. At least 200 infected cells were examined for each experiment, and data are mean ± s.d. from three replicates. A two-tailed unpaired Student's *t*-test was performed (*$P < 0.05$; **$P < 0.01$). **e**,**f**, Membrane localization of the substrates is required for their modification by IcsB. 293T cells were co-transfected with IcsB and an indicated Flag-tagged substrate. The mutants assayed in **e** are cysteine mutants devoid of lipid modification or deletion of the transmembrane helix for VAMP8 (D76–96). **f**, RhoA, Rab13 and VAMP8 mutants with or without the PBR, both of which bear a single modifiable lysine, were assayed. Cells were metabolized with Alk-16 and harvested for in-gel fluorescence assay. Data (**b**–**f**) are representative of three independent experiments.

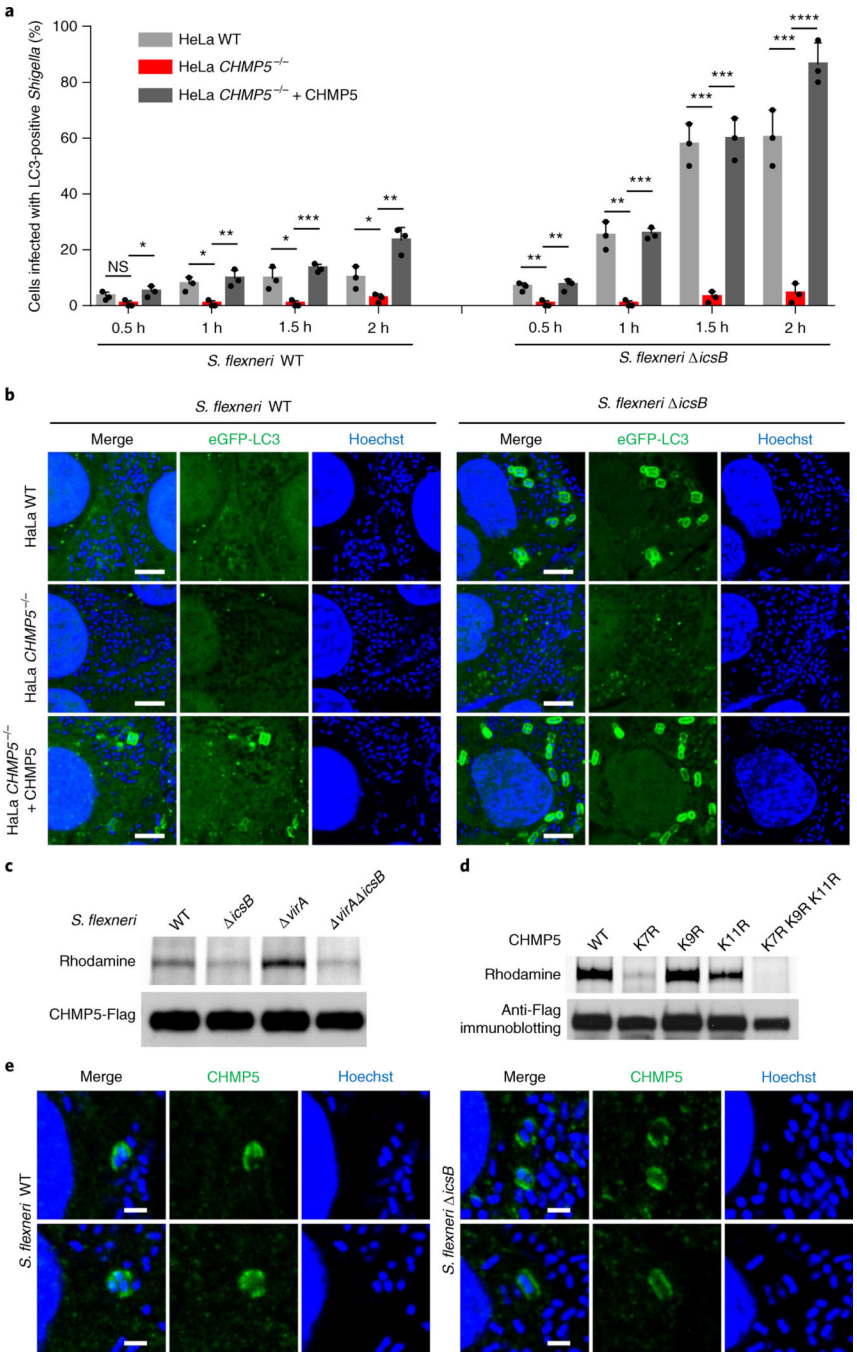

Fig. 6 |. Fatty acylation of CHMP5 by IcsB is important for *Shigella* escape from host autophagy.

a,**b**, Effects of *CHMP5* deficiency on bacterial autophagosome formation in response to *S. flexneri* infection. Indicated HeLa cells expressing eGFP-LC3 were infected with *S. flexneri* WT or Δ*icsB*. **a**, Percentages of infected cells containing LC3-positive *S. flexneri* at indicated time points after infection. **b**, Representative fluorescence images taken at 2 h post-infection (scale bars, 3 μm). At least 200 infected cells were examined for each experiment and the data are means ± s.d. from three replicates. A two-tailed unpaired Student's *t*-test was performed (**P*< 0.05; ***P*< 0.01; ****P*< 0.001; *****P*< 0.0001; NS, 0.0734). **c**,

Stearoylation of CHMP5 by IcsB during *S. flexneri* infection. 293T cells stably expressing Flag-CHMP5 were infected with *S. flexneri* WT, Δ*icsB*, Δ *virA* or Δ *virA*Δ *icsB* in the presence of Alk-16. Cells were harvested 2 h after infection for in-gel fluorescence assay. **d**, Effects of lysine mutation on CHMP5 stearoylation by IcsB. 293T cells were transfected with IcsB and Flag-CHMP5 (WT or an indicated K to R mutant). Cells were metabolized with Alk-16 for 24 h and subjected to in-gel fluorescence assay. **e**, Localization of endogenous CHMP5 by immunofluorescence staining in *S. flexneri*-infected HeLa cells (scale bars, 1 μm). Data shown in **a**–**e** are representative of three independent experiments.

Nat Microbiol. Author manuscript; available in PMC 2019 April 16.

Table 1 |

IcsB substrates identified in chemical proteomic screens

Protein symbol	IcsB transfection	*S. flexneri* WT infection	*S. flexneri* Δ*virA* infection	Loss of function test	Lipidation	Classification
RHOA, RHOC, RHOG, RAC1	√	√	√	Knockout	*	Rho family
RHOF		√	√	Knockout	*	
RAC2	√			Not tested	*	
CDC42		√	√	Knockout	*	
H-RAS, K-RAS, R-RAS, RAP1B	√	√	√	Knockout	*	Ras family
RALA	√	√	√	Not tested	*	
RALB	√	√		Not tested	*	
RAP1A		√	√	Knockout	*	
RHEB	√			Not tested	*	
RAB8A, RAB11A, RAB11B, RAB13, RAB22A, RAB23, RAB34, RAB35	√	√	√	Knockout	*	Rab family
RAB5B	√		√	Not tested	*	
RAB6A		√		Knockout	*	
RAB6B		√		Knockout	*	
RAB9A		√	√	Knockout	*	
RAB39A		√		Not tested	*	
YKT6	√	√	√	RNAi (85%)	*	SNARE
VAMP3	√			RNAi (89%)		
VAMP8	√	√	√	Knockout		
BNIP1	√			Not tested		
SEC22B	√			RNAi (95%)		
SEPT2		√		Not tested		Septin
SEPT7	√	√	√	RNAi (70%)		
SEPT9		√		Not tested		
SEPT11		√	√	Knockout		
CHMP5	√	√	√	Knockout		
CHMP4B	√			Not tested		
BASP1	√	√	√	Not tested	*	

Protein symbol	IcsB transfection	*S. flexneri* WT infection	*S. flexneri* Δ*virA* infection	Loss of function test	Lipidation	Classification
MARCKS	√	√	√	Knockout	*	
MARCKSL1	√	√	√	Not tested	*	
CNP	√	√	√	Knockout	*	
GNG12	√	√		Not tested	*	
CD44		√	√	Knockout		
CDCP1		√	√	Not tested		
DSG2		√	√	Knockout		
FNBP1L		√	√	Knockout		
WASL		√	√	Not tested		
TRIP10		√	√	Knockout		
FERMT2			√	Not tested		
EPS8			√	Not tested		
EPS8L2		√		Not tested		
S100A13	√			Not tested		
PTRF	√			Not tested		
GIPC1	√			Not tested		
FKBP8	√			RNAi (95%)		
FKBP11	√			Not tested		
EPB41L2	√			Not tested		
EPB41L1	√			Not tested		

RNAi, RNA interference.